



Diffusion weighted imaging evidence of extra-callosal pathways for interhemispheric communication after complete commissurotomy

Jason S. Nomi¹ · Emily Marshall¹ · Eran Zaidel^{2,3} · Bharat Biswal⁴ · F. Xavier Castellanos^{5,6} · Anthony Steven Dick⁷ · Lucina Q. Uddin^{1,8} · Eric Mooshagian⁹

Received: 31 August 2018 / Accepted: 20 March 2019 / Published online: 7 May 2019
© Springer-Verlag GmbH Germany, part of Springer Nature 2019

Abstract

The integrity of white matter architecture in the human brain is related to cognitive processing abilities. The corpus callosum is the largest white matter bundle interconnecting the two cerebral hemispheres. “Split-brain” patients in whom all cortical commissures have been severed to alleviate intractable epilepsy demonstrate remarkably intact cognitive abilities despite the lack of this important interhemispheric pathway. While it has often been speculated that there are compensatory alterations in the remaining interhemispheric fibers in split-brain patients several years post-commissurotomy, this has never been directly shown. Here we examined extra-callosal pathways for interhemispheric communication in the brain of a patient who underwent complete cerebral commissurotomy using diffusion weighted imaging tractography. We found that compared with a healthy age-matched comparison group, the split-brain patient exhibited increased fractional anisotropy (FA) of the dorsal and ventral pontine decussations of the cortico-cerebellar interhemispheric pathways. Few differences were observed between the patient and the comparison group with respect to FA of other long-range intrahemispheric fibers. These results point to specific cerebellar anatomical substrates that may account for the spared interhemispheric coordination and intact cognitive abilities that have been extensively documented in this unique patient.

Keywords Corpus callosum · Structural connectivity · Interhemispheric transfer · Epilepsy · Hemispheric specialization · Laterality

Jason S. Nomi, Emily Marshall, Lucina Q. Uddin and Eric Mooshagian contributed equally to the manuscript.

✉ Jason S. Nomi
jxn131@miami.edu

✉ Lucina Q. Uddin
l.uddin@miami.edu

¹ Department of Psychology, University of Miami, P.O. Box 248185-0751, Coral Gables, FL 33124, USA

² Department of Psychology, University of California, Los Angeles, CA 90095, USA

³ Brain Research Institute, University of California, Los Angeles, CA 90095, USA

⁴ Department of Biomedical Engineering, New Jersey Institute of Technology, Newark, NJ 07102, USA

⁵ Department of Child and Adolescent Psychiatry, Hassenfeld Children’s Hospital at NYU Langone, New York, NY 10016, USA

⁶ Nathan Kline Institute for Psychiatric Research, Orangeburg, NY 10962, USA

⁷ Department of Psychology, Florida International University, Miami, FL 33199, USA

⁸ Neuroscience Program, University of Miami Miller School of Medicine, Miami, FL 33136, USA

⁹ Department of Neuroscience, Washington University School of Medicine, Saint Louis, MO 63110, USA

Introduction

Brain function emerges from its structure. Human cognitive processing abilities depend on the integrity of white matter architecture, and white matter lesions result in the classic disconnection syndromes (Geschwind 1965). The corpus callosum (CC) is the principal white matter bundle in the brain, comprising axons responsible for fast interhemispheric transfer and integration between the cerebral hemispheres. Yet, commissurotomy, or “split-brain”, patients in whom the major forebrain commissures have been sectioned to prevent the spread of epileptic seizures, demonstrate remarkably intact cognitive abilities (Bogen et al. 1965).

Only careful tachistoscopic testing reveals deficits in interhemispheric transfer in split-brain patients. Decades of behavioral testing has documented that even complete commissurotomy patients can engage in cognitive processes requiring interhemispheric coordination. Here we discuss patient N.G., who underwent complete forebrain commissurotomy in 1963 to relieve intractable epilepsy. The surgery involved sectioning of the CC, anterior commissure, hippocampal commissure, and massa intermedia. In subsequent post-surgery testing on a simple reaction time task, patient N.G. showed evidence of subcallosal transfer of visual information that was sensitive to the eccentricity of the stimuli in the two visual fields, but not to their intensities (Clarke and Zaidel 1989). Presenting letter stimuli to both hemispheres of commissurotomy patient N.G., Eviatar and Zaidel demonstrated that the patient could cross-compare letters presented bilaterally, providing additional evidence for subcallosal transfer of visual information (Eviatar and Zaidel 1994). Further evidence suggests that patient N.G. has an unusual ability to cross compare even complex visual stimuli across the vertical meridian. In a test using Vanderplas figures, created to be neither verbal nor easily verbalizable, N.G. again demonstrated interhemispheric visual transfer by performing above chance when asked to compare shapes presented to both visual fields (Clarke and Zaidel 1994).

Residual, albeit degraded, interhemispheric transfer and integration in certain domains suggests that commissurotomy patients may accomplish interhemispheric coordination via alternative interhemispheric pathways. Theoretical models of sensory-motor interhemispheric transfer in the split-brain include routes involving the brainstem and ipsilateral motor pathways. Subcortical interhemispheric communication has long been posited to support a range of transfer abilities in commissurotomy patients (Clarke and Zaidel 1989). The precise anatomical pathways involved, however, have not yet been delineated.

Possible intact interhemispheric pathways of communication in patients with complete commissurotomy include the cortico-ponto-cerebellar loop (CPCL) and

dentate-rubro-thalamic tract (DRTT) (Keser et al. 2015). The CPCL consists of afferent cerebellar fibers connecting frontal, parietal, and visual cortex to the thalamus that then connect to the cerebellum via pontine decussations of the middle cerebellar peduncles (MCP). Cortico-ponto-cerebellar pathways have been reconstructed in the human brain using diffusion tractography and are posited to play a role in cognition (Palesi et al. 2017). The DRTT consists of efferent cerebellar fibers that connect the dentate nucleus to a mid-brain decussation via the superior cerebellar peduncles that then connects to the thalamus and outer cortex. While motor functions of the cerebellum are well documented (Shadmehr 2017), this brain structure is also involved in language (Vias and Dick 2017), emotional processing (Adamaszek et al. 2017), and executive function (Bellebaum and Daum 2007), leading to theories that cerebro-cerebellar loops serve a broader role in adaptive prediction for motor and cognitive function (Sokolov et al. 2017). Given the complete lack of cortical interhemispheric fibers in the complete commissurotomy patient, the CPCL and DRTT may be the only pathways that can support the preserved interhemispheric coordination observed in these individuals.

Diffusion weighted imaging (DWI) provides a method for the noninvasive tracking of white matter paths. DWI analyses allow one to quantify the magnitude and direction of water diffusion, thereby inferring the existence of underlying white matter microstructure. Diffusion tensor imaging (DTI) is the most commonly used approach to analyze DWI data. DTI allows for the computation of fractional anisotropy (FA), which reflects both myelination and organization of white matter fibers. FA information can be exploited to trace white matter tract trajectories, as diffusion of water molecules is hindered by the axonal membrane and myelin sheath. Water molecules disperse primarily in the direction of the fiber tract, allowing one to infer the overall orientation of white matter fibers.

In the present analysis, we describe diffusion tractography results from a complete commissurotomy patient, N.G., previously demonstrated to exhibit largely intact interhemispheric functional connectivity in the absence of residual transcallosal fibers approximately 45 years post-surgery (Uddin et al. 2008). We examined whether surgical section of the CC and other forebrain commissures results in observable changes in white matter architecture of cerebellar peduncle fibers and brain stem decussations forming parts of the CPCL and DRTT. We focused on these fibers and decussations specifically, as we reasoned these would be the areas where interhemispheric transfer of information could potentially occur. We could not be sure whether intrahemispheric fibers would be affected as a result of lifetime compensatory reorganization after commissurotomy. Thus, we also evaluated several major intrahemispheric fibers including the arcuate fasciculus (AF), uncinate fasciculus (UF), and the cingulum bundle (CB) in both the patient and a group

of age-matched individuals. We found evidence of substantial changes in FA of spared inter- but not intrahemispheric extra-callosal pathways in patient N.G., specifically in the dorsal and ventral pontine decussations. These findings demonstrate possible cortico-cerebellar mechanisms supporting preserved interhemispheric communication in patient N.G.

Experimental procedures

Participants

We analyzed neuroimaging data collected from patient N.G., a right-handed woman (74 years of age at time of data acquisition) who underwent complete forebrain commissurotomy in 1963. The surgery consisted of single-stage midline section of the anterior commissure, corpus callosum, hippocampal commissure, and massa intermedia. A complete case history is reported in Bogen et al. (1965). Previous reports document that this patient sustained greater preoperative extracallosal structural damage to the right hemisphere (Campbell et al. 1981). This damage is evident in the patient's structural MRI. Behavioral testing has indicated some preserved interhemispheric interaction as indexed by various neuropsychological tests (Campbell et al. 1981). Preoperative and postoperative full-scale IQ was 76 and 71, respectively. This study was approved by the IRB at the University of Arizona and New York University School of Medicine. Informed consent was obtained from the patient according to the Declaration of Helsinki, and she was compensated for her participation.

A group of 20 individuals (14 female) were randomly chosen as a comparison group based on age and the availability of diffusion weighted MRI data from a publicly available dataset (Enhanced Nathan Kline Institute–Rockland Sample (Nooner et al. 2012)). The average age of participants in this group was 72.7 years ($SD = 3.16$; range = 68–79) and the average full-scale IQ was 117.35 ($SD = 16.51$; range = 78–141). Seventeen participants had positive laterality scores (above 75), indicating right-hand preference, and three had negative scores (–25, –70, –55), indicating left-hand preference, as measured by the Edinburgh Handedness Questionnaire (Oldfield 1971). Thus, the comparison group was age-matched to the patient, although IQ- and handedness-matching could not be achieved. Informed consent was obtained from all individuals according to the Declaration of Helsinki, and they were compensated for participation.

Data acquisition

Neuroimaging data for the split-brain patient was acquired on a General Electric 3.0 T HD Signa Excite scanner (General Electric, Milwaukee, Wisconsin, USA) equipped with Optimized ACGD Gradients located at the University of Arizona. Along with other functional images not discussed in the current study (Uddin et al. 2008), a T1-weighted anatomical image (Magnetization Prepared Rapid Gradient Echo, TR = 2500 ms; TE = 4.35 ms; TI = 900 ms; flip angle = 8°; 176 slices; FOV = 256 mm) and a 25-direction diffusion MRI sequence were acquired (TR = 13,000 ms; TE = 72.1 ms; flip angle = 90°; matrix 128 × 128; FOV = 256 mm; 3-mm slices; 2 × 2 × 3-mm voxels; b value = 1000).

Neuroimaging data for the comparison group were acquired on a Siemens Trio TM 3.0 T MRI scanner (http://fcon_1000.projects.nitrc.org/indi/enhanced/) (Nooner et al. 2012). The current study used the T1 structural image (TR/TE = 1900/2.52 ms; FOV = 250 mm; 1 × 1 × 1 mm voxels; AP phase encoding) and a multiband (acceleration factor = 4) 137-direction diffusion weighted image (TR/TE = 2400/85 ms; FOV = 212; 2 × 2 × 2 mm voxels; AP phase encoding; b value = 1500) for each subject.

Data preprocessing

All diffusion MRI data were preprocessed in native subject space using the Tolerably Obsessive Registration and Tensor Optimization Indolent Software Ensemble (TORTOISE) software package (<https://science.nichd.nih.gov/confluence/display/nihpd/TORTOISE>) that is freely available from the National Institutes of Health (Pierpaoli et al. 2010). Preprocessing steps in TORTOISE used the DIFFPREP function and included motion and eddy current distortion correction with B-matrix reorientation and B0 susceptibility induced EPI distortion correction. Structural T1 weighted images were skull-stripped using the BET function in FSL (Jenkinson et al. 2005; Smith 2002) and were matched with the B0 image to correct for EPI distortions using TORTOISE.

General tractography procedure

Diffusion tensors were reconstructed in native subject space from the preprocessed data using DSI studio software (<http://dsi-studio.labsolver.org>). Each fiber tract was estimated using a deterministic streamline-tracking algorithm in both directions along the principal diffusion axis (Yeh et al. 2013). Briefly, for each tract of interest, a spherical mask was placed in the white matter. In some cases, additional mask regions were also used to delineate a specific tract. When extraneous tracks were visible, a region-of-absence (ROA) mask was used to constrain the algorithm

so that only fibers passing through the tracts of interest were retained. Path tracing proceeded until FA fell below 0.2 or until the minimum angle between the current and previous path segments was larger than 35° . Minimum and maximum tract lengths were set at 30 mm and 500 mm, respectively. To account for different voxel sizes between the two data sets, the step size (between 0.1 and 3 mm) and smoothing (between 0 and 95%) were varied using a deterministically random algorithm. Accordingly, a large number of initializations (1,000,000) were employed to ensure enough iterations of the step-size and smoothing algorithms. Increasing the number of initializations has also been shown to reduce tract variability (Cheng et al. 2012). These procedures were taken to help reduce differences between datasets (e.g., voxel size, number of directions).

Interhemispheric fiber tracking

First, we sought to confirm the lack of residual transcallosal fibers in patient N.G. First, a whole brain seed was used to identify all tracts throughout the brain using a FA threshold of > 0.20 . Second, CC ROIs from the FreeSurfer Segmentation atlas within DSI studio (https://surfer.nmr.mgh.harvard.edu/fswiki/mri_cc) were normalized to the patient's brain. This atlas includes five ROIs that divide the corpus callosum into anterior, mid-anterior, central, mid-posterior and posterior regions. Fiber tracking for each ROI was then performed using the same tracking parameters

and general protocol used to identify the other white matter tracts examined.

Figure 1 shows the white matter mask placements for each of the fiber bundles examined. Cerebellar tracts were identified using a modified version of the protocol described by Leitner and colleagues (Leitner et al. 2015). The MCPs are found at the level of the pons in the brainstem and form a portion of the CPCL. For the dorsal and ventral bands of the MCP, a single spherical ROI was placed within each of the dorsal and ventral pontine decussations to identify the dorsal and ventral MCP bands (Fig. 1a). ROAs were placed superior and inferior to the MCP bands in axial slices. Diffusion metrics were calculated for the dorsal and ventral pontine decussation ROIs and for the dorsal and ventral MCP bands.

The superior cerebellar peduncle (SCP) tracts run bilaterally in a diagonal manner (inferior-posterior to superior-anterior) and form part of the DRTT. For the SCP, a spherical ROI was placed within the dentate nucleus at the level of the medial pons (Fig. 1b). A second spherical ROI was placed near the decussation of the SCPs near the pontomesencephalic junction. A spherical ROA was placed superior to the SCP decussation to remove associated corticospinal tracts. As in previous research, we could not reliably track the SCP decussation along with the SCP for all subjects (Leitner et al. 2015). Thus, the tract was terminated before entering the SCP decussation. This procedure was repeated for the left- and right-SCP.

Fig. 1 ROI and seed placement for tracking of the **a** middle and **b** superior cerebellar peduncles, **c** arcuate fasciculus, **d** uncinate fasciculus, **e** cingulum bundle. Mask placement is shown in axial view. ROAs (red) were used occasionally to prevent outlier tracts

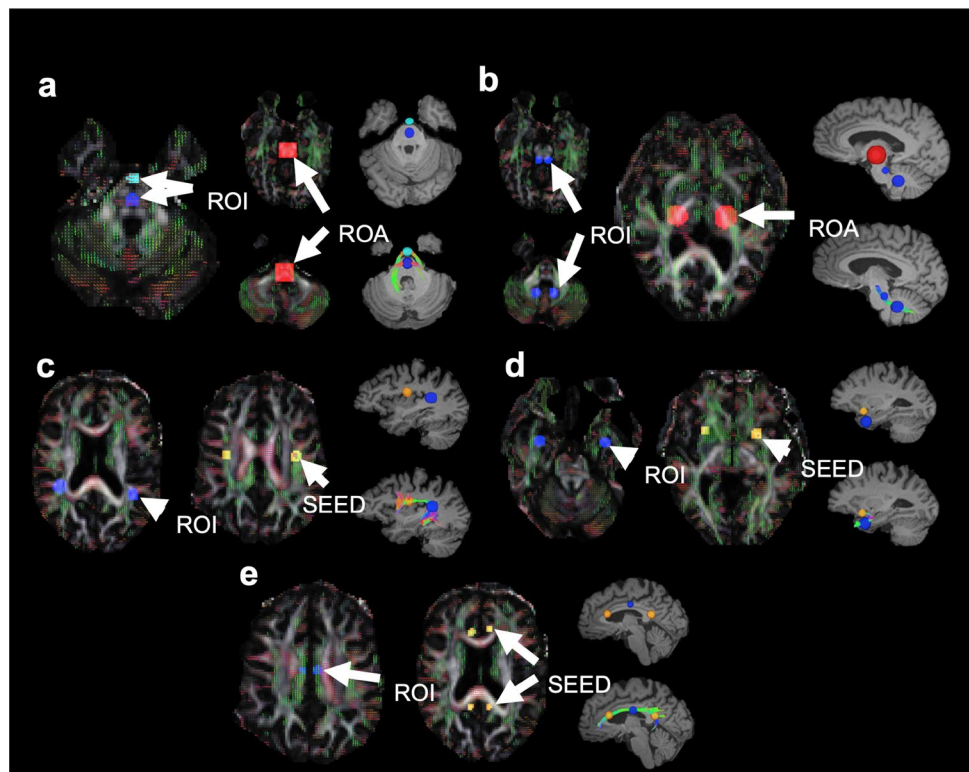
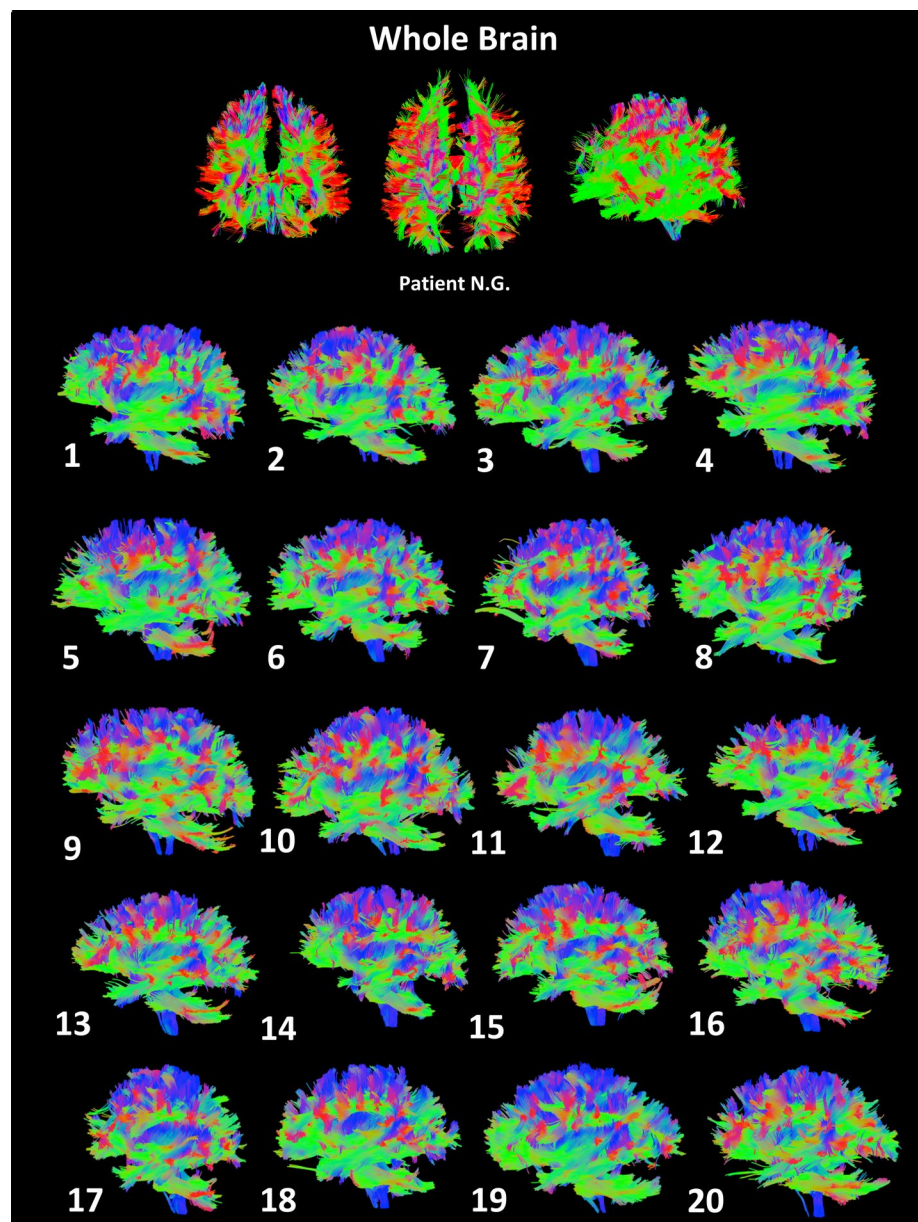


Fig. 2 Whole-brain tractography for split-brain patient N.G. (top) and each of the 20 comparison subjects (bottom). Patient data are shown in coronal (top left), axial (top middle), and sagittal (top right) views. Comparison subject data are shown in lateral view. Colors represent tract orientation: Red = left/right, blue = dorsal/ventral, green = anterior/posterior



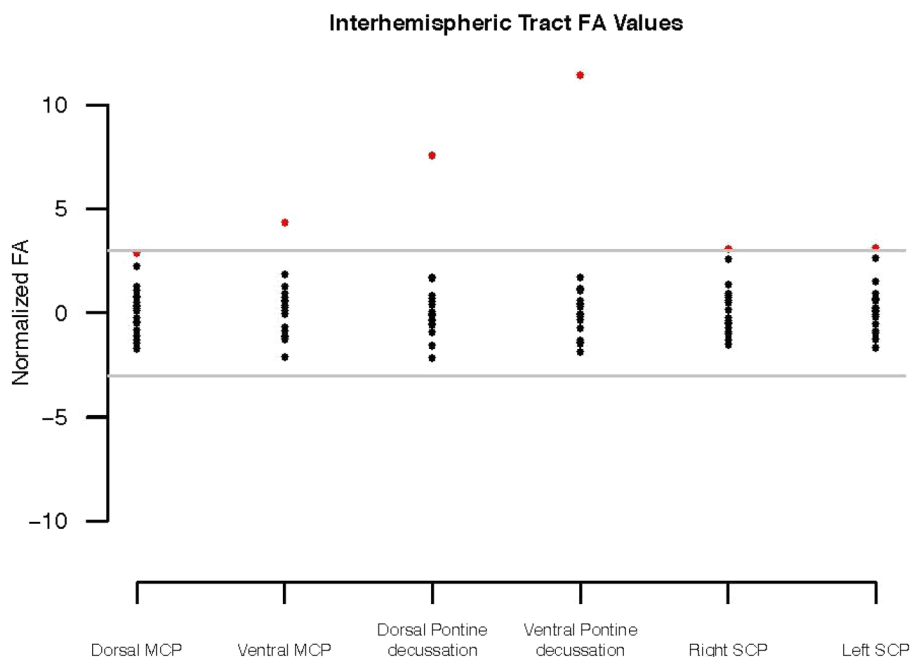
Intrahemispheric fiber tracking

Intrahemispheric fiber tracking focused on the bilateral AF, UF, and CB. The AF connects inferior frontal, parietal and temporal cortex within each hemisphere. The AF was identified using a spherical ROI placed near the “elbow” point of the AF close to the temporo-parietal junction, using the sagittal and axial planes to orient along the superior-inferior and medial–lateral axes; respectively (Fig. 1c) (Propper et al. 2010). A spherical seed was then placed on the superior branch of the AF near the pre- and postcentral gyri. If any extraneous tracts were produced, an additional spherical ROA was placed at the level of the lateral sulcus between the superior and inferior sections of the AF.

The UF is present bilaterally, and connects the inferior frontal and anterior temporal cortex within each hemisphere. To identify the UF, a spherical seed was placed just below the elbow of the UF within the anterior temporal lobe (Fig. 1d) (Rodrigo et al. 2007). An ROI was placed near the inferior frontal cortex at the level of the lateral sulcus and anterior commissure. If any extraneous tracts were produced, an additional ROA was placed posterior to the elbow of the UF.

The CB runs bilaterally along the superior part of the corpus callosum and connects frontal, parietal, and medial temporal brain areas. The CB was identified by placing one spherical seed near the genu and another spherical seed near the splenium of the corpus callosum using the sagittal plane

Fig. 3 Z-transformed inter-hemispheric FA values for split-brain patient N.G. (red) and comparison subjects (black) in each of six interhemispheric fiber tracts. Each dot denotes a single subject. Upper and lower horizontal gray lines denote the ± 3 SD. *MCP* middle cerebellar peduncle, *SCP* superior cerebellar peduncle



to orient in the superior–inferior axis and the axial plane to orient in the medial–lateral axis. An ROI was placed at the midpoint between the initial two seeds (Fig. 1e) (Jones et al. 2013).

Fiber tract quantification

The primary measure of interest was mean FA of each fiber tract. FA is a measure of the directional nature of water diffusion and is associated with various structural properties of the underlying white matter (Beaulieu 2002). The mean FA value for each tract for each subject was computed as follows: First, a whole-brain ROI was used to compute the whole-brain average FA value. Then, the FA value for each tract was divided by the whole brain value to produce a normalized measure accounting for individual differences in overall FA. Next, the FA mean and standard deviation (SD) for each tract were calculated across all control participants. Then, the values were converted to z -scores for each control individual and for patient N.G. based on the mean and SD of the comparison group. We used a threshold of ± 3 SD of the mean of the comparison group values to determine if metrics for N.G. were within the normal distribution. Note that the comparison group's non-normalized FA values for the whole brain, all ROIs, and all tracts were normally distributed as determined by the Shapiro–Wilk test (all p values > 0.05).

Results

Whole-brain FA

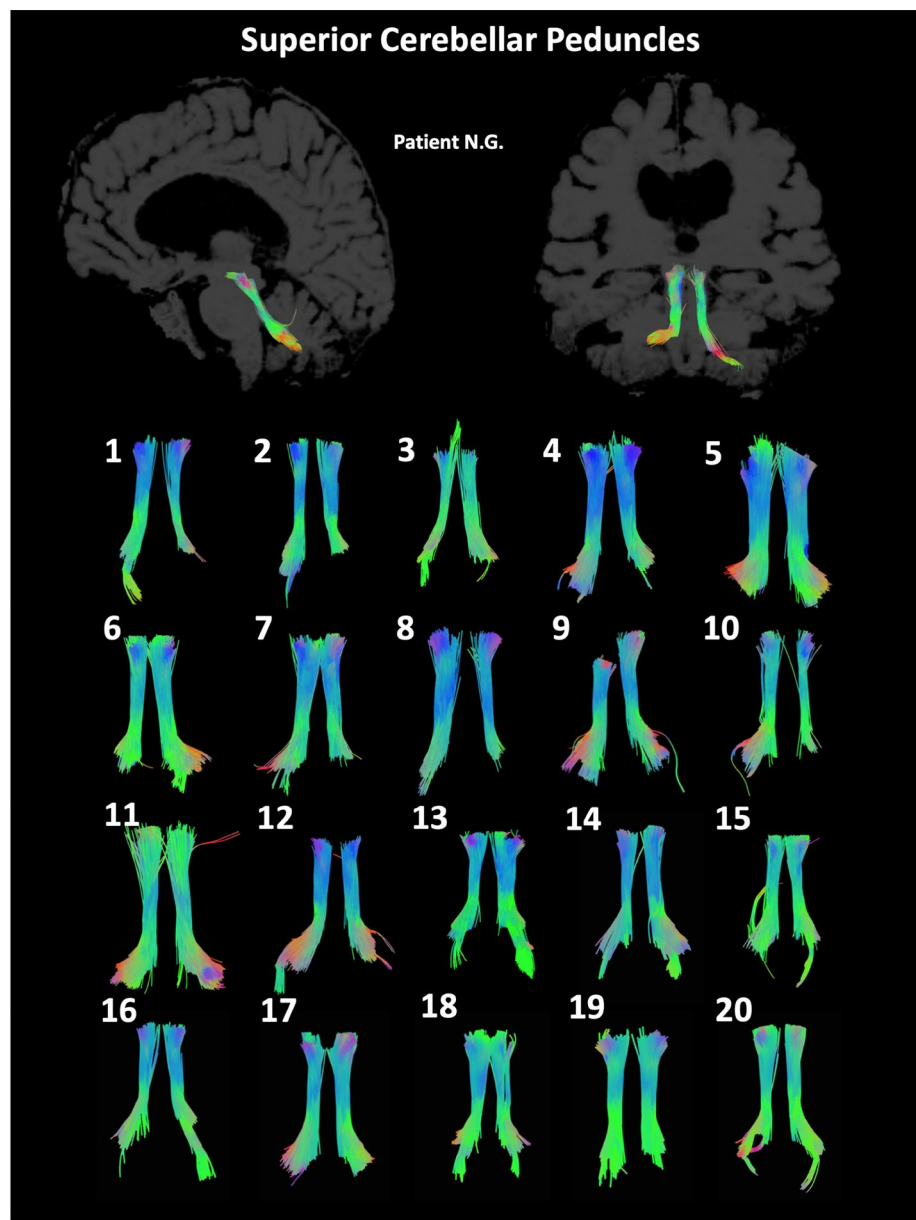
We compared N.G.'s whole-brain average FA to the comparison group (Fig. 2). N.G.'s whole-brain average FA fell within the range of the comparison group average FA (SD = +1.77).

Interhemispheric fiber tracts

In order to confirm that there were no residual transcallosal fibers in patient N.G., we examined both whole brain fiber tracking and fiber tracking using CC ROIs. As expected, these regions did not yield any detectable fibers interconnecting the cerebral hemispheres in patient N.G., confirming the completeness of the commissurotomy procedure [Fig. 2, see also (Uddin et al. 2008)].

The cerebellar peduncle fibers and associated decussations of the brainstem were the main tracts of interest. Due to the complete cerebral commissurotomy of N.G., we hypothesized that these brain structures would show substantial increases in FA compared with the comparison group. Figure 3 shows the mean FA values for each of the comparison subjects and patient N.G., for each decussation and interhemispheric tract. N.G. had higher FA values for the left and right SCP (3.59 and 3.09 SD, respectively; Fig. 4). FA was elevated compared with the comparison group in both the ventral and dorsal MCP (4.61 SD and 2.80 SD, respectively), though only surpassed the 3 SD threshold for the ventral tract. N.G.'s FA was most

Fig. 4 Superior cerebellar peduncle tracts for patient N.G. (top) and each of the 20 comparison subjects (bottom)



increased in the ventral and dorsal pontine decussation ROIs (11.29 and 7.33 SD, respectively; Fig. 5). The high FA values observed in N.G.'s brainstem decussations provide evidence for possible alternate routes of interhemispheric communication that may have reorganized as a compensatory mechanism post-commissurotomy.

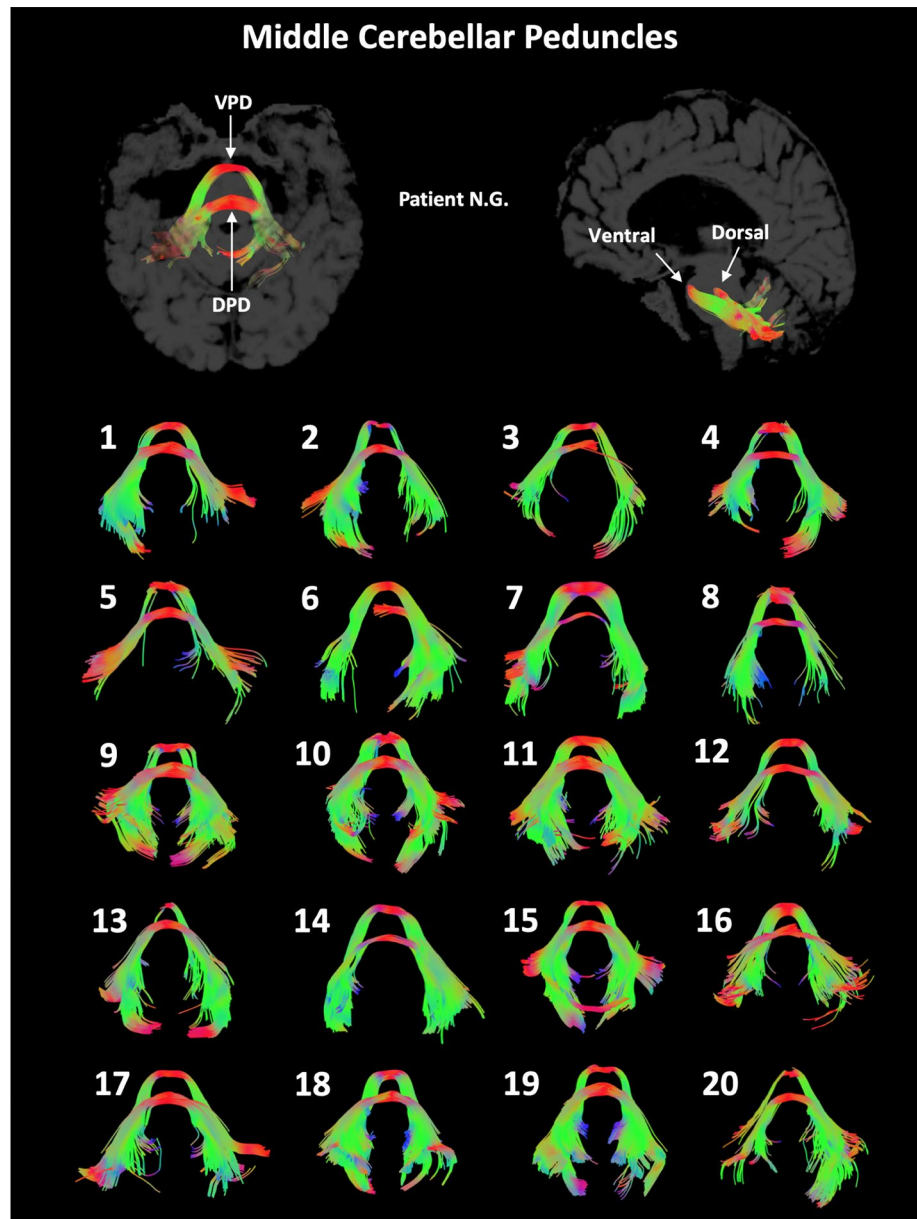
Intrahemispheric fiber tracts

Major intrahemispheric fiber pathways were examined to determine the specificity of reorganization of N.G.'s white matter pathways. We also sought to demonstrate that increased interhemispheric water diffusion was not due

solely to different acquisition parameters, as the patient data were collected on a different MRI scanner than the comparison data.

Figure 6 shows the mean FA values for each of the comparison subjects and patient N.G., for each intrahemispheric tract. Patient N.G.'s FA for intrahemispheric fiber bundles fell within the comparison range (within ± 3 SD) for the left and right UF (1.72 SD and 0.23 SD, respectively; Fig. 7) and the left and right AF (-1.59 SD and -0.67 SD, respectively; Fig. 8) fiber bundles. In contrast, N.G. exhibited lower FA values for the left and right CB fiber bundle (-2.83 SD and -4.86 SD, respectively; Fig. 9). The CB is located near the corpus callosum and may have been affected by

Fig. 5 Middle cerebellar peduncle tracts for patient N.G. (top) and each of the 20 comparison subjects (bottom). *VPD* ventral pontine decussation, *DPD* dorsal pontine decussation



her commissurotomy (Campbell et al. 1981). This is especially evident for her right CB, where it can be seen that the tract stops prematurely around the pre-central gyrus instead of continuing anteriorly towards the genu of the corpus callosum.

In summary, we show that in split-brain patient N.G., the FA of cerebellar decussations was higher than expected given values observed in an age-matched comparison group, whereas FA values for most major intrahemispheric fibers remained within the expected range.

Discussion

The classic callosal disconnection syndrome describes the phenomenon that split-brain patients can no longer verbally identify stimuli presented to the left visual field, as this information is processed by the non-verbal right hemisphere that has been cut off from the verbal left hemisphere. Despite such deficits that can be observed with careful tachistoscopic lateralized stimulus presentation, split-brain patients demonstrate “a remarkable absence of functional impairment in nearly all ordinary behavior” (Bogen et al. 1965). Patient N.G. in particular displayed a range of abilities post-commissurotomy that were indicative of partially preserved

Fig. 6 Z-transformed intrahemispheric FA values for split-brain patient N.G. (red) and comparison subjects (black) for each of six intrahemispheric fiber tracts. Each dot denotes a single subject. Upper and lower horizontal gray lines denote the ± 3 SD. *AF* arcuate fasciculus, *UF* uncinate fasciculus, *CB* cingulate bundle

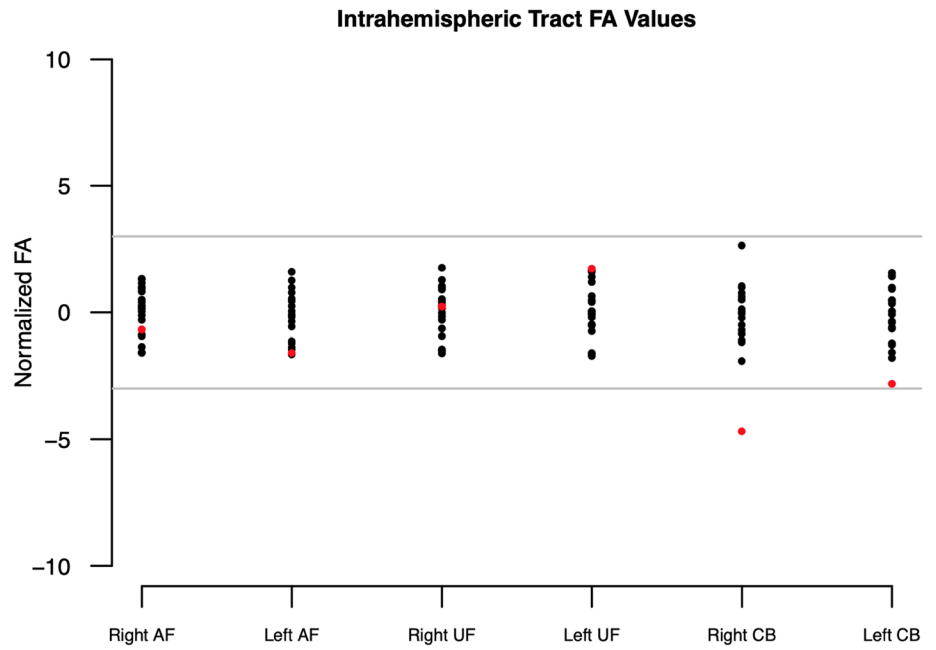


Fig. 7 Uncinate fasciculus tracts for patient N.G. (top) and 20 comparison subjects (bottom). *L* left hemisphere, *R* right hemisphere

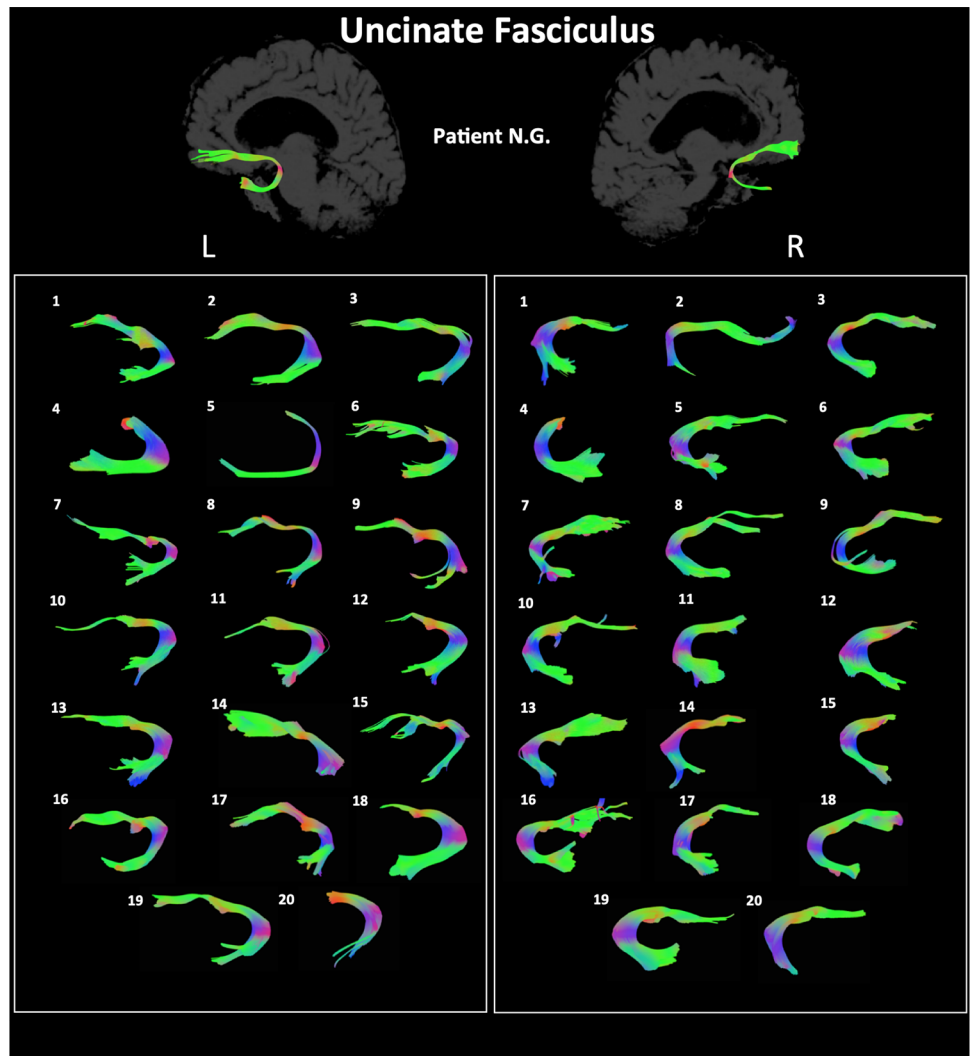
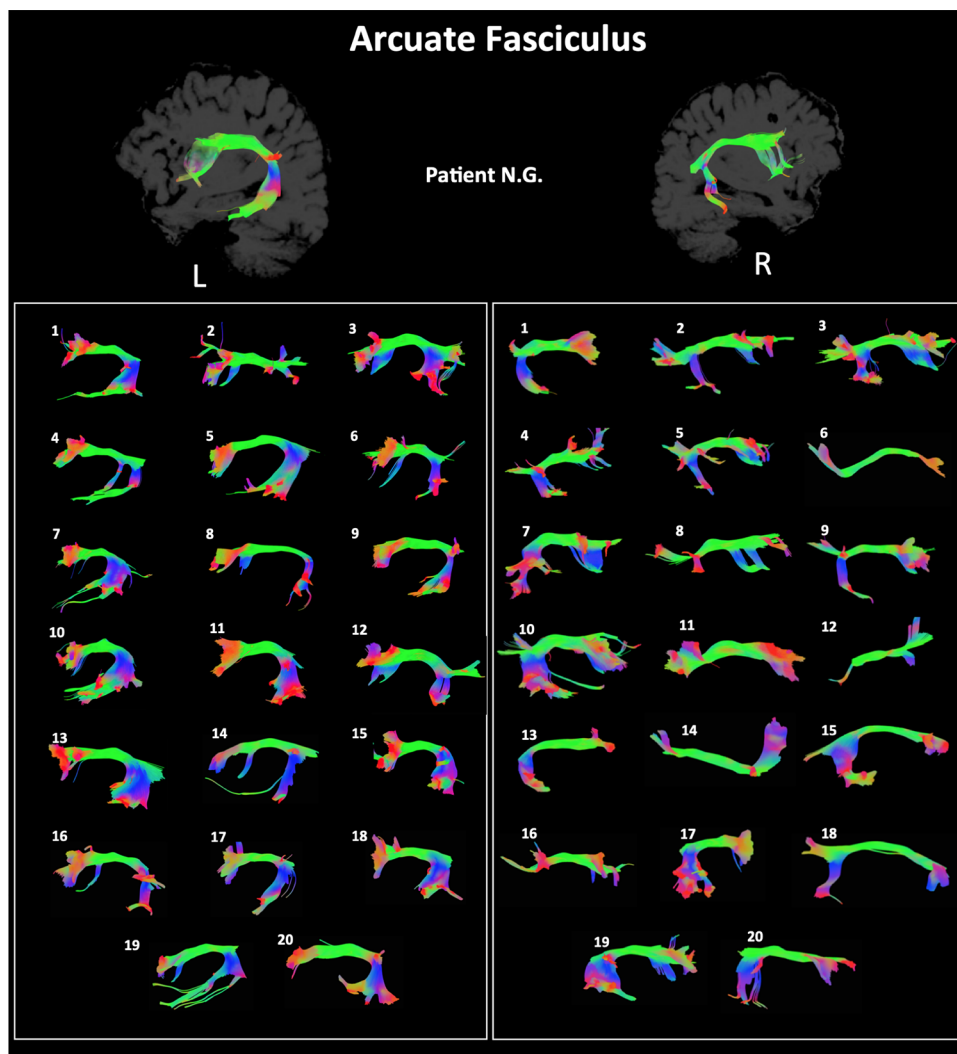


Fig. 8 Arcuate fasciculus tracts for patient N.G. (top) and each of the 20 comparison subjects (bottom). *L* left hemisphere, *R* right hemisphere



interhemispheric communication. A series of behavioral experiments testing simple reaction time (Clarke and Zaidel 1989), letter comparison (Eviatar and Zaidel 1994), and comparison of other complex non-verbal visual stimuli (Clarke and Zaidel 1994) demonstrated that she could cross-compare visual shapes across the vertical meridian. Thus, decades of behavioral research and observations of partially intact interhemispheric transfer in split-brain patients have led to the speculation that subcortical interhemispheric connections maintain communication between the hemispheres in the absence of cerebral commissures. Until now, no physical evidence of these purported compensatory anatomical pathways has been described. Further, the long-term sequelae of complete commissurotomy has not previously been explored.

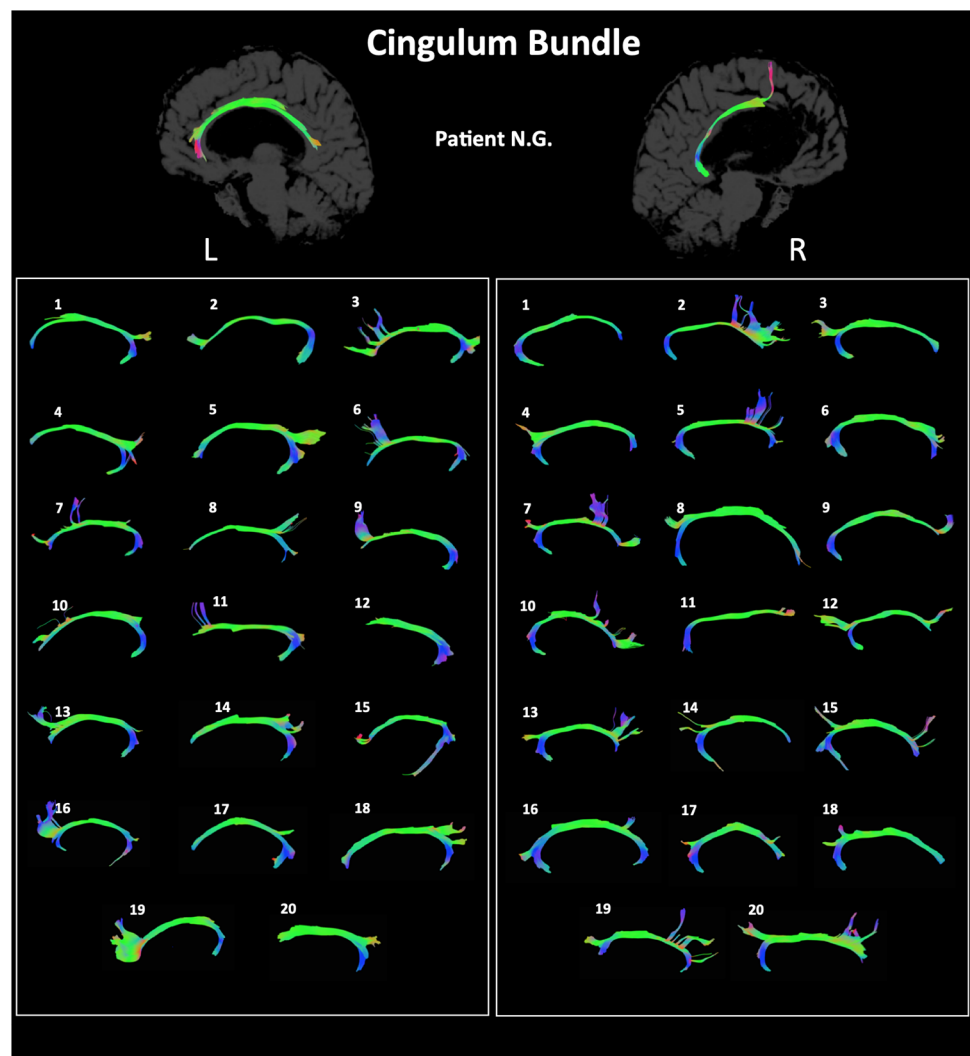
Here we present the first evidence for structural interhemispheric compensation within extra-callosal subcortical pathways in a commissurotomy patient. Specifically, we find that the middle and superior cerebellar peduncles

giving rise to the pontine decussations of patient N.G. exhibit higher FA compared with age-matched comparison participants.

The possibility that residual transcallosal fibers exist or have regrown in patient N.G. is unlikely for several reasons. First, the completeness of the surgical section of all cerebral commissures in this patient was previously demonstrated over 20 years post-surgery using MRI (Bogen et al. 1988). Second, our own DWI data show no evidence of any such fibers (Fig. 2). More generally, though white matter plasticity is observed in the peripheral nervous system, it is very limited in the central nervous system tracts like those under study here (Huebner and Strittmatter 2009). This suggests that whatever extra-callosal mechanisms are mediating interhemispheric coordination post-surgery must be subcortical.

In the absence of callosal fibers connecting cortical regions in the two hemispheres, information must travel long distances via intrahemispheric tracts before it is transferred to the opposite hemisphere via subcortical tracts. White

Fig. 9 Cingulum bundle tracts for patient N.G. (top) and each of the 20 comparison subjects (bottom). *L* left hemisphere, *R* right hemisphere



matter tracts have been shown to exhibit experience-dependent changes (Scholz et al. 2009). Given this, one might have expected to observe an increase in FA for intrahemispheric fiber bundles necessary to transmit information to subcortical tracts like the cerebellar peduncles. However, we did not observe such changes in the patient examined. Instead, FA values for N.G. fell within the range of the comparison group for the UF and AF tracts and were significantly decreased in the right CB tracts. Thus, instead of overall changes in intrahemispheric or whole brain FA, only particular fibers capable of maintaining interhemispheric coordination were specifically altered.

Interestingly, FA within the right CB tracts was much lower for N.G. than for age-matched comparison individuals, perhaps reflecting damage to the cingulate cortex that occurred during surgery (Campbell et al. 1981). Indeed, this damage can be observed in the sagittal view of the MRI of the patient. The fact that this damage to the CB can be assessed and quantified using DWI further supports the

claim that it is possible to identify changes to specific fiber tracts post-surgery in this patient.

We and others have previously explored potential compensatory mechanisms for interhemispheric transfer in the split-brain using functional connectivity (FC) measures applied to resting state fMRI data. We demonstrated that patient N.G. shows evidence for bilateral resting state functional connectivity, with interhemispheric correlation scores falling within the comparison range for most brain regions examined. Of note, interhemispheric FC was particularly high between posterior brain regions for this patient (Uddin et al. 2008). Other work, however, has revealed that functional connectivity between the hemispheres is significantly reduced immediately after commissurotomy in both humans (Johnston et al. 2008; Roland et al. 2017) and monkeys (O'Reilly et al. 2013). In humans, the significant reduction in FC has been shown to persist to at least 7 years post-surgery (Roland et al. 2017). In our patient, neuroimaging data were collected

over 40 years post-surgery, suggesting that a lifetime of experience may have contributed to the observed recovery of functional connectivity in addition to compensatory subcortical structural connectivity. Relationships between functional and structural connectivity in the brain are complex, and may change across the lifespan (Honey et al. 2009; Uddin 2013; Uddin et al. 2011). The current results point to the critical need for long-term follow up of patients who have undergone drastic neurosurgical procedures both for patient prognosis and for contributing to our understanding of structure–function relationships in the brain.

Limitations

We contend that the most likely explanation for the observed cerebellar white matter differences in this patient is reorganization in response to the surgery. However, given the lack of pre-surgical diffusion MRI data, we cannot say so with certainty. It is possible that atypical white matter was present prior to surgery. Additionally, this study was conducted in only one patient. The diffusion data were acquired at a single time point over 40 years post-surgery.

The patient and comparison data were collected on different scanners with different acquisition parameters. However, the similarity of FA values for whole-brain and intra-hemispheric fiber tracts observed between the patient and comparison individuals indicates that differences between the patient and comparison data observed with respect to interhemispheric fibers are not necessarily attributable to these discrepancies.

A final limitation of the current study is that we were only able to obtain low-resolution DWI data from patient N.G., and consequently only FA measures were computed. It is well documented that FA is highly susceptible to crossing fibers (Jeurissen et al. 2013; Ruddy et al. 2017). In the current analyses, the fiber tracts most likely to be affected by this limitation are the lateral projections of the corpus callosum and the pontocerebellar fibers. The use of diffusion spectrum imaging in future studies will be necessary to resolve these ambiguities (Wedeen et al. 2008).

Conclusion

The claim that subcortical pathways mediate transfer of information between the hemispheres after complete commissurotomy has never been verified anatomically. We find evidence for higher FA of dorsal and ventral pontine decussations in commissurotomy patient N.G. compared with age-matched comparison individuals, suggesting a

very specific potential extra-callosal interhemispheric transfer location in this patient. These findings point to the existence of a previously unknown subcortical anatomical substrate that we hypothesize may contribute to preserved interhemispheric communication in these remarkable patients.

Acknowledgements The authors thank Anouk Scheres and Scott Squire for assistance with data collection.

Funding This work was supported by a University of Miami Gabelli Senior Scholar Award, an award from the Canadian Institute for Advanced Research, and National Institute of Mental Health [R01MH107549] to LQU. We also acknowledge the Nathan Kline Institute Enhanced Rockland Sample for the availability of age-matched comparison participants, collected with support from R01MH094639.

Compliance with ethical standards

Conflict of interest The authors declare that they have no conflict of interest.

Ethical approval All procedures performed in studies involving human participants were in accordance with the ethical standards of the institutional and/or national research committee and with the 1964 Helsinki declaration and its later amendments or comparable ethical standards. This article does not contain any studies with animals performed by any of the authors.

References

- Adamaszek M, D'Agata F, Ferrucci R, Habas C, Keulen S, Kirkby KC, Leggio M, Marien P, Molinari M, Moulton E, Orsi L, Van Overwalle F, Papadelis C, Priori A, Sacchetti B, Schutter DJ, Styliadis C, Verhoeven J (2017) Consensus paper: cerebellum and emotion. *Cerebellum* 16(2):552–576. <https://doi.org/10.1007/s12311-016-0815-8>
- Beaulieu C (2002) The basis of anisotropic water diffusion in the nervous system—a technical review. *NMR Biomed* 15(7–8):435–455. <https://doi.org/10.1002/nbm.782>
- Bellebaum C, Daum I (2007) Cerebellar involvement in executive control. *Cerebellum* 6(3):184–192. <https://doi.org/10.1080/14734220601169707>
- Bogen JE, Fisher ED, Vogel PJ (1965) Cerebral commissurotomy. A second case report. *JAMA* 194(12):1328–1329
- Bogen JE, Schultz DH, Vogel PJ (1988) Completeness of callosotomy shown by magnetic resonance imaging in the long term. *Arch Neurol* 45(11):1203–1205
- Campbell AL Jr, Bogen JE, Smith A (1981) Disorganization and reorganization of cognitive and sensorimotor functions in cerebral commissurotomy. Compensatory roles of the forebrain commissures and cerebral hemispheres in man. *Brain* 104(3):493–511
- Cheng H, Wang Y, Sheng J, Sporns O, Kronenberger WG, Mathews VP, Hummer TA, Saykin AJ (2012) Optimization of seed density in DTI tractography for structural networks. *J Neurosci Methods* 203(1):264–272. <https://doi.org/10.1016/j.jneumeth.2011.09.021>
- Clarke JM, Zaidel E (1989) Simple reaction times to lateralized light flashes. Varieties of interhemispheric communication routes. *Brain* 112(Pt 4):849–870

- Clarke JM, Zaidel E (1994) Anatomical-behavioral relationships: corpus callosum morphometry and hemispheric specialization. *Behav Brain Res* 64(1–2):185–202
- Eviatar Z, Zaidel E (1994) Letter matching within and between the disconnected hemispheres. *Brain Cogn* 25(1):128–137
- Geschwind N (1965) Disconnexion syndromes in animals and man. I. *Brain* 88(2):237–294
- Honey CJ, Sporns O, Cammoun L, Gigandet X, Thiran JP, Meuli R, Hagmann P (2009) Predicting human resting-state functional connectivity from structural connectivity. *Proc Natl Acad Sci USA* 106(6):2035–2040
- Huebner EA, Strittmatter SM (2009) Axon regeneration in the peripheral and central nervous systems. *Results Probl Cell Differ* 48:339–351. https://doi.org/10.1007/400_2009_19
- Jenkinson M, Pechaud M, Smith S (2005) BET2: MR-based estimation of brain, skull and scalp surfaces. In: 11th annual meeting of the organization for human brain mapping, Toronto
- Jeurissen B, Leemans A, Tournier JD, Jones DK, Sijbers J (2013) Investigating the prevalence of complex fiber configurations in white matter tissue with diffusion magnetic resonance imaging. *Hum Brain Mapp* 34(11):2747–2766. <https://doi.org/10.1002/hbm.22099>
- Johnston JM, Vaishnavi SN, Smyth MD, Zhang D, He BJ, Zempel JM, Shimony JS, Snyder AZ, Raichle ME (2008) Loss of resting interhemispheric functional connectivity after complete section of the corpus callosum. *J Neurosci* 28(25):6453–6458. <https://doi.org/10.1523/jneurosci.0573-08.2008>
- Jones DK, Christiansen KF, Chapman RJ, Aggleton JP (2013) Distinct subdivisions of the cingulum bundle revealed by diffusion MRI fibre tracking: implications for neuropsychological investigations. *Neuropsychologia* 51(1):67–78. <https://doi.org/10.1016/j.neuropsychologia.2012.11.018>
- Keser Z, Hasan KM, Mwangi BI, Kamali A, Ucisik-Keser FE, Riasec RF, Yozbatiran N, Francisco GE, Narayana PA (2015) Diffusion tensor imaging of the human cerebellar pathways and their interplay with cerebral macrostructure. *Front Neuroanat* 9:41. <https://doi.org/10.3389/fnana.2015.00041>
- Leitner Y, Travis KE, Ben-Shachar M, Yeom KW, Feldman HM (2015) Tract profiles of the cerebellar white matter pathways in children and adolescents. *Cerebellum* 14(6):613–623. <https://doi.org/10.1007/s12311-015-0652-1>
- Nooner KB, Colcombe SJ, Tobe RH, Mennes M, Benedict MM, Moreno AL, Panek LJ, Brown S, Zavitz ST, Li Q, Sikka S, Gutman D, Bangaru S, Schlachter RT, Kamiel SM, Anwar AR, Hinz CM, Kaplan MS, Rachlin AB, Adelsberg S, Cheung B, Khanuja R, Yan C, Craddock CC, Calhoun V, Courtney W, King M, Wood D, Cox CL, Kelly AM, Di Martino A, Petkova E, Reiss PT, Duan N, Thomsen D, Biswal B, Coffey B, Hoptman MJ, Javitt DC, Pomara N, Sidtis JJ, Koplewicz HS, Castellanos FX, Leventhal BL, Milham MP (2012) The NKI-rockland sample: a model for accelerating the pace of discovery science in psychiatry. *Front Neurosci* 6:152. <https://doi.org/10.3389/fnins.2012.00152>
- Oldfield RC (1971) The assessment and analysis of handedness: the Edinburgh Inventory. *Neuropsychologia* 9:97–113
- O'Reilly JX, Crosson PL, Jbabdi S, Sallet J, Noonan MP, Mars RB, Browning PG, Wilson CR, Mitchell AS, Miller KL, Rushworth MF, Baxter MG (2013) Causal effect of disconnection lesions on interhemispheric functional connectivity in rhesus monkeys. *Proc Natl Acad Sci USA* 110(34):13982–13987. <https://doi.org/10.1073/pnas.1305062110>
- Palesi F, De Rinaldis A, Castellazzi G, Calamante F, Muhlert N, Chard D, Tournier JD, Magenes G, D'Angelo E, Gandini Wheeler-Kingshott CAM (2017) Contralateral cortico-ponto-cerebellar pathways reconstruction in humans in vivo: implications for reciprocal cerebro-cerebellar structural connectivity in motor and non-motor areas. *Sci Rep* 7(1):12841. <https://doi.org/10.1038/s41598-017-13079-8>
- Propper RE, O'Donnell LJ, Whalen S, Tie Y, Norton IH, Suarez RO, Zollei L, Radmanesh A, Golby AJ (2010) A combined fMRI and DTI examination of functional language lateralization and arcuate fasciculus structure: effects of degree versus direction of hand preference. *Brain Cogn* 73(2):85–92. <https://doi.org/10.1016/j.bandc.2010.03.004>
- Rodrigo S, Oppenheim C, Chassoux F, Golestani N, Cointepas Y, Poupon C, Semah F, Mangin JF, Le Bihan D, Meder JF (2007) Uncinate fasciculus fiber tracking in mesial temporal lobe epilepsy. Initial findings. *Eur Radiol* 17(7):1663–1668. <https://doi.org/10.1007/s00330-006-0558-x>
- Roland JL, Snyder AZ, Hacker CD, Mitra A, Shimony JS, Limbrick DD, Raichle ME, Smyth MD, Leuthardt EC (2017) On the role of the corpus callosum in interhemispheric functional connectivity in humans. *Proc Natl Acad Sci USA* 114(50):13278–13283. <https://doi.org/10.1073/pnas.1707050114>
- Ruddy KL, Leemans A, Carson RG (2017) Transcallosal connectivity of the human cortical motor network. *Brain Struct Funct* 222(3):1243–1252. <https://doi.org/10.1007/s00429-016-1274-1>
- Scholz J, Klein MC, Behrens TE, Johansen-Berg H (2009) Training induces changes in white-matter architecture. *Nat Neurosci* 12(11):1370–1371. <https://doi.org/10.1038/nn.2412>
- Shadmehr R (2017) Distinct neural circuits for control of movement vs. holding still. *J Neurophysiol* 117(4):1431–1460. <https://doi.org/10.1152/jn.00840.2016>
- Smith SM (2002) Fast robust automated brain extraction. *Hum Brain Mapp* 17(3):143–155. <https://doi.org/10.1002/hbm.10062>
- Sokolov AA, Miall RC, Ivry RB (2017) The cerebellum: adaptive prediction for movement and cognition. *Trends Cogn Sci* 21(5):313–332. <https://doi.org/10.1016/j.tics.2017.02.005>
- Uddin LQ (2013) Complex relationships between structural and functional brain connectivity. *Trends Cogn Sci* 17(12):600–602. <https://doi.org/10.1016/j.tics.2013.09.011>
- Uddin LQ, Mooshagian E, Zaidel E, Scheres A, Margulies DS, Kelly AM, Shehzad Z, Adelstein JS, Castellanos FX, Biswal BB, Milham MP (2008) Residual functional connectivity in the split-brain revealed with resting-state functional MRI. *NeuroReport* 19(7):703–709. <https://doi.org/10.1097/WNR.0b013e3282fb8203>
- Uddin LQ, Supekar KS, Ryali S, Menon V (2011) Dynamic reconfiguration of structural and functional connectivity across core neurocognitive brain networks with development. *J Neurosci* 31(50):18578–18589. <https://doi.org/10.1523/JNEUROSCI.4465-11.2011>
- Vias C, Dick AS (2017) Cerebellar contributions to language in typical and atypical development: a review. *Dev Neuropsychol* 42(6):404–421. <https://doi.org/10.1080/87565641.2017.1334783>
- Wedeen VJ, Wang RP, Schmahmann JD, Benner T, Tseng WY, Dai G, Pandya DN, Hagmann P, D'Arceuil H, de Crespigny AJ (2008) Diffusion spectrum magnetic resonance imaging (DSI) tractography of crossing fibers. *NeuroImage* 41(4):1267–1277. <https://doi.org/10.1016/j.neuroimage.2008.03.036>
- Yeh FC, Verstynen TD, Wang Y, Fernandez-Miranda JC, Tseng WY (2013) Deterministic diffusion fiber tracking improved by quantitative anisotropy. *PLoS One* 8(11):e80713. <https://doi.org/10.1371/journal.pone.0080713>